Proc. Natl. Acad. Sci. USA
Vol. 96, pp. 8493–8498, July 1999
Cell Biology

Retention of the Bub3 checkpoint protein on lagging chromosomes

MARIA J. MARTINEZ-EXPOSITO*, KENNETH B. KAPLAN*, JAY COPELAND, AND PETER K. SORGER†

Department of Biology, 68–371, Massachusetts Institute of Technology, 77 Massachusetts Avenue, Cambridge, MA 02139

Communicated by Stephen C. Harrison, Harvard University, Cambridge, MA, April 14, 1999 (received for review December 16, 1998)

ABSTRACT **Accurate chromosome segregation at mitosis is ensured both by the intrinsic fidelity of the mitotic machinery and by the operation of checkpoints that monitor chromosome-microtubule attachment. When unattached kinetochores are present, anaphase is delayed and the time available for chromosome-microtubule capture increases. Genes required for this delay first were identified in budding yeast (the *MAD* and *BUB* genes), but it is not yet known how the checkpoint senses unattached chromosomes or how it signals cell-cycle arrest. We report the isolation and analysis of a murine homologue of *BUB3*, a gene whose deletion abolishes mitotic checkpoint function in *Saccharomyces cerevisiae*. mBub3 belongs to a small gene family that has been highly conserved through evolution. By expressing recombinant proteins in insect cells, we show that mBub3, like yeast Bub3p, binds to Bub1 to form a complex with protein kinase activity. During prophase and prometaphase, preceding kinetochore-microtubule attachment, Bub3 localizes to kinetochores. High levels of mBub3 remain associated with lagging chromosomes but not with correctly aligned chromosomes during metaphase, consistent with a role for Bub3 in sensing microtubule attachment. Intriguingly, the number of lagging chromosomes with high Bub3 staining increases dramatically in cells treated with low (and pharmacologically relevant) concentrations of the chemotherapeutic taxol and the microtubule poison nocodazole.**

The accurate segregation of chromosomes requires that all pairs of sister chromatids achieve a state of bivalent attachment to the mitotic spindle before the onset of anaphase (1). Bivalent attachment occurs when one kinetochore on a pair of sister chromatids is attached to microtubules emanating from one spindle pole and the other kinetochore is attached to microtubules emanating from the opposite pole. A checkpoint monitors kinetochore-microtubule interaction and delays cell cycle progression until all chromosome attachments are bivalent (2–4).

It seems likely that checkpoint lesions play an important role in tumorigenesis. The frequent occurrence of aneuploidy in tumor cells and the association of whole-chromosome loss of heterozygosity with the development of several types of cancers suggest that error-prone chromosome segregation may give rise to a mutator phenotype and thereby promote tumor development (5–7). This possibility is strengthened by the finding that a human checkpoint gene (*Bub1*; ref. 3) is mutated in some human colorectal cancers (8).

Genes required for the mitotic checkpoint first were identified in budding yeast. The *Saccharomyces cerevisiae MAD1–3* and *BUB1–3* genes are not required for cell viability, but mutations in these genes abolish mitotic delay in response to unattached kinetochores, increase the rate of chromosome loss, and raise the sensitivity of cells to antimicrotubule drugs (9, 10). The isolation of mammalian homologues of Mad2 and Bub1 has shown that these proteins are present on unattached kinetochores (11–14), and dominant negative mutants and antibody microinjection (14–16) have implicated the proteins in the control of chromosome segregation. In this paper we report the isolation and analysis of the murine Bub3 gene. We find that murine Bub3, like yeast Bub3p, binds to Bub1 to form an active kinase complex (17). mBub3 is present on unattached kinetochores and, in cells treated with very low concentrations of taxol, it is selectively retained on lagging chromosomes.

MATERIALS AND METHODS

DNA, Cell Culture, and Protein Methods. A screen by hybridization of a day 10 mouse embryo cDNA library with radio-labeled DNA from two murine expressed sequence tags (ESTs), Genbank accession nos. W11868 and W13647, yielded 19 positive phages. The insert in one subclone of the phage (clone 20a) appeared to be full length, containing a 1,350-bp insert with an ATG at bp 57, an ORF 30% identical to yBub3, and a poly(A) tail. Overall, mBub3 is identical to two recently described human Bub3 proteins over 325 of its first 326 residues, but is unlike either hBUB3 in its final amino acid (two independent mBUB3 clones were confirmed to have the same C terminus). This similarity is not a consequence of cross-species contamination in the libraries because 89 silent DNA differences are present between human and mouse.

HeLa cells were grown in media containing 10% FBS. Nocodazole and taxol were added fresh from stocks in DMSO. Mitotic cells were isolated by first arresting the cells at the G_1/S boundary via a double thymidine block, releasing them for 14–16 hr, and harvesting them by shake-off (18).

mBub1 and *mBub3* genes were cloned into the pFastBac baculovirus expression vector (Life Technologies, Grand Island, NY) and fused to an amino terminal His_{10}HA epitope tag. Recombinant viruses were obtained and used to infect HI5 insect cells essentially as described (19).

Antibodies against mBub1 and mBub3 were obtained by immunizing rabbits with keyhole limpet hemocyanin-conjugated 14 aa peptides comprising Bub3 residues 207–221 (SPO14), 313–327 (SPO15), or Bub1 158–172 (each rabbit was immunized with a single peptide). Western blots were quantitated by using a PhosphorImager after incubation with primary antibodies and ^{125}I protein A.

Microscopy Methods. For immunofluorescence, cells grown on coverslips were fixed with 3.7% paraformaldehyde for 20 min at room temperature, permeabilized with 0.1% Triton X-100/PBS for 7 min, blocked with 0.2% gelatin in PBS/0.02% NaN3 for 20 min, and incubated for 20 min with raw or affinity-purified anti-Bub3 antisera, mouse monoclonal anti-β tubulin (TUB 2.1 from Sigma), and human CREST serum at 1:1,000. Cells then were washed three times with 0.2% gelatin-PBS and 0.02% sodium azide, incubated for 20 min, and then stained with 4′,6-diamidino-2-phenylindole and with affinity-purified FITC or Texas Red-conjugated goat anti-rabbit or

The publication costs of this article were defrayed in part by page charge payment. This article must therefore be hereby marked "*advertisement*" in accordance with 18 U.S.C. §1734 solely to indicate this fact.

PNAS is available online at www.pnas.org.

Abbreviations: EST, expressed sequence tag; HA, hemagglutinin; 3D, three-dimensional.

*M.J.M.-E. and K.B.K. contributed equally to this work.
†To whom reprint requests should be addressed. e-mail: psorger@mit.edu.

goat anti-mouse, or FITC-conjugated goat anti-human (Santa Cruz Biotechnology). Alternatively, cells in suspension were recovered by centrifugation, fixed, and stained in solution, then applied to slides in mounting solution. The specificity of anti-Bub3 antibodies was demonstrated by incubation with a 70-fold excess of either immunizing or nonspecific peptides for 1 hr on ice before use.

Immunostained specimens were examined by using a 63× Plan-apochromat objective, 0.2-μm thick Z-sections, and a Princeton Instruments Quantix cooled charge-coupled device camera on a Ziess-Applied Precision DeltaVision Restoration microscope. Exposures were chosen that yielded 200–1,800 gray scale units, remaining well above the camera dark current but below the 4,096-unit maximum. To create three-dimensional (3D) models, two-dimensional polygons were first constructed on each Z-section, one fluor at a time, based on intensity levels chosen to highlight structural boundaries. The stacks of two-dimensional polygons then were rendered into 3D objects, and images of the models were enhanced by adjusting the transparency and false color of the rendered 3D objects.

RESULTS

Isolation of a Murine Bub3 Gene and its mRae1 Homologue. A search of Genbank for ESTs yielded one murine EST with significant sequence similarity to yeast Bub1 and two ESTs with similarity to yeast Bub3. When DNA from these ESTs was used to screen mouse embryonic cDNA libraries, we isolated a kinase identical in sequence to the mBub1 gene recently reported by Taylor and McKeon (14) and a second gene (clone 20a) encoding a 326-residue protein 29% identical to *S. cerevisiae Bub3* (Fig. 1; ref. 17). BLAST analysis with clone 20a revealed a closely related murine gene (which we will call *mRae1*) encoding a 368-aa protein 30% identical to clone 20a and about 40% identical to *Schizosaccharomyces pombe Rae1* and *S. cerevisiae GLE2* (20, 21). Our murine sequence data, combined with Genbank sequences, yielded a phylogentic tree showing that all six eukaryotes examined contained one Bub3-like and one Rae1-like gene (Fig. 1*a*); in no organism were additional genes found that were more than 10% identical. Although Bub3 and Rae1 contain WD40 motifs, the regions of similarity between the two proteins extends well beyond the WD40 domains (Fig. 1 *b* and *c*). We therefore conclude that Rae1 and Bub3 are members of a gene family in which there are two branches. Whereas yeast Bub3 is involved in the mitotic checkpoint (17, 22), Rae1 and Gle2p appear to be involved in nuclear-cytoplasmic transport (20, 21, 23).

Physical Association of mBub1 and mBub3 in an Active Kinase Complex. Yeast Bub3p binds to yeast Bub1p (17) and dominant-negative fragments of murine Bub1 have been shown to disrupt the mitotic checkpoint and prevent nocodazole-mediated apoptosis (14). To link mBub3 functionally to the mitotic checkpoint in animal cells, we asked whether mBub1 and mBub3 would associate to form a complex with protein kinase activity. Hemagglutinin (HA)-tagged mBub1 and mBub3 proteins were coexpressed in insect cells by using baculovirus vectors. Whole-cell extracts were prepared, HA-mBub1 or HA-mBub3 were immunoprecipitated by using polyclonal antibodies raised against either mBub1 or mBub3-derived peptides, and the levels of HA-mBub1 and HA-mBub3 in the immunoprecipitates were determined by anti-HA immunoblotting (Fig. 2*A*). Immune complexes isolated with anti-mBub1 sera contained both mBub1 and mBub3; immune complexes isolated with anti-mBub3 sera contained both mBub3 and mBub1. In both cases, immunoprecipitation was blocked by the addition of excess immunizing but not nonspecific peptides (Fig. 2*A* and data not shown). Bub1-Bub3 immune complexes appear to contain similar amounts of the two proteins, as judged by blotting, and Bub1 was active in autophosphorylation when incubated with γ-^{32}P-ATP (Fig. 2*B*). We conclude that mBub1 and mBub3 associate to form

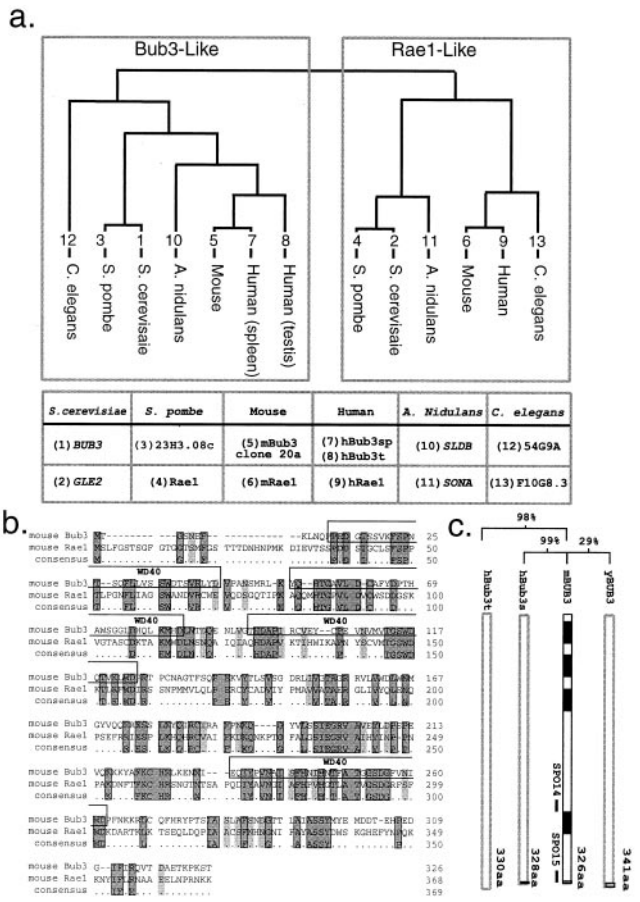

FIG. 1. Sequence analysis of Bub3 and Rae1. (*a*) A tree generated by PHYLIP (45) comparing sequences listed below and aligned with CLUSTAL. Branch lengths are arbitrary, but the connectivity was robust. *Bub3* and *Rae1* genes from different organisms were obtained as follows: 1) Sc-Bub3, accession number M64707 (17); 2) Sc-Gle2, U18839 (20), 3) Sp-23H3.08c, Z99163; 4) Sp-Rae1, U14951 (21); 5) m-Bub3 (this work); 6, m-Rae1 (this work and ref. 23); 7) h-Bub3, AF053304 for spleen and 8) AF047473 for testis; 9) h-Rae1, U84720 (23); 10) An-SLDB, AF032988 (43); 11) An-SONA, AF069492 (44); 12) Ce-54G9A, AL032648 (l); 13) Ce-F10G8.3, Z80216. (*b*) Sequence alignment of mouse Bub3 and Rae1 with boxes around four putative WD40 domains (46). (c) Schematic of yeast, mouse, and two human Bub3 proteins showing percent identity and the positions of the SPO14 and SPO15 peptides. Dark boxes denote WD40 repeats.

a complex with kinase activity. It has been suggested that yeast Bub3p may activate Bub1p (17), but we have not observed activation of mBub1 by mBub3 in insect cells (Fig. 2, lanes 6 and 11), either because mBub1 is intrinsically active or because recombinant mBub1 associates with, and is activated by, endogenous insect-cell Bub3.

Bub3 Is Present at High Levels on Kinetochores Lacking Bound Microtubules. To determine the subcellular localization of Bub3, HeLa, 3T3, and PtK2 cells were stained with polyclonal antisera raised against either of two different mBub3 peptides and imaged with a DeltaVision Restoration Microscope (Issaquah, WA) (24). In all cell types examined, anti-Bub3 antibodies recognized a single band on Western blots with an apparent molecular mass of 40 kDa (Fig. 2*C* and data not shown). Preliminary experiments showed that HeLa cells contained the highest levels of Bub3, and they were used for subsequent experiments; the protein sequences of murine and human Bub3 are identical in the regions used to prepare antipeptide antibodies, so that same antisera can be used in both organisms. In prophase and prometaphase cells, bright hBub3 staining was visible at discrete points along chromo-

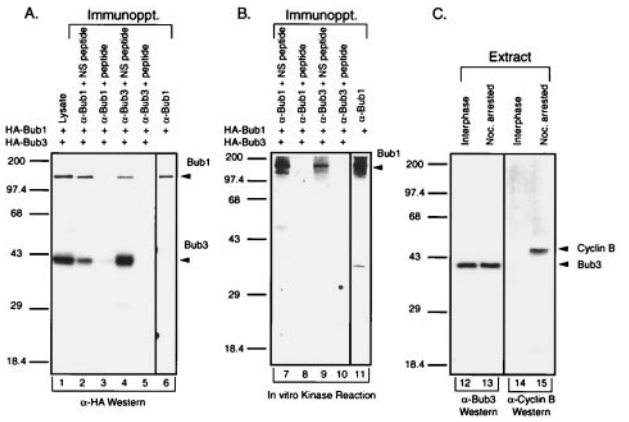

FIG. 2. Active mBub1 kinase associates with mBub3. (*A*) Recombinant mBub1 and mBub3 coimmunoprecipitate. Lysates from insect cells coexpressing HIS_{10}HA-Bub1 and HIS_{10}HA-Bub3 or expressing HIS_{10}HA-Bub1 alone were analyzed by using antipeptide antibodies against either mBub1 (lanes 2, 3, and 6) or mBub3 (lanes 4 and 5). A 20-fold molar excess of nonspecific (lanes 2 and 4) or specific peptide (lanes 3 and 5) were added as specificity controls. (*B*) Protein kinase activity of mBub1. Immune complexes containing HIS_{10}HA-Bub1 and HIS_{10}HA-Bub3 (lanes 7–10) or HIS_{10}HA-Bub1 alone (lane 11) were prepared as in *A* and incubated with ^{32}P-γ-ATP at room temperature for 30 min in kinase buffer before analysis by autoradiography. (*C*) hBub3 is present at similar levels in interphase and mitotic HeLa cells. Fifty micrograms of extract from interphase (lanes 12 and 14) or nocodazole-treated (lanes 13 and 15) cells were analyzed by Western blotting using anti-Bub3 or anti-cyclin B antibodies.

somes (Fig. 3 *A* and *B*) and diffusely in the cytosol. This punctate staining colocalized with antikinetochore staining generated by CREST antisera (25) and with fluorescent *in situ* hybridization signals generated by alpha-satellite probes (Fig. 3*E*; alpha-satellite is a major component of human centromeres). Thus, endogenous Bub3 is associated with the kinetochores of mitotic chromosomes, as has recently been reported for transfected human Bub3 tagged with green fluorescent protein (22).

In HeLa, PtK2, and 3T3 cells, the highest levels of kinetochore-associated Bub3 were observed in prophase and prometaphase; metaphase chromosomes stained significantly less intensely (Fig. 3*D* and data not shown). When HeLa cells were treated with nocodazole for 18 hr, kinetochore-associated Bub3 rose to very high levels (Fig. 3*F*). This increase reflected differences in the extent of Bub3-kinetochore association rather than changes in the intracellular concentration of Bub3, as judged by Western blotting (Fig. 2*C*; lanes 12 and 13). We were concerned that differences in the intensity of Bub3 at kinetochores in untreated and nocodazole-arrested cells (or in prophase and metaphase cells) might arise artifactually if microtubule-kinetochore association inhibited hBub3-antibodies binding. To examine this, we synchronized and then released HeLa cells from S phase, waited until the majority of the cells were in metaphase, and then added chilled media containing nocodazole. The nocodazole in the media rapidly depolymerized microtubules and low temperatures slowed other intracellular processes, presumably yielding metaphase-like kinetochores lacking bound microtubules. Before nocodazole treatment, 20% of the synchronized HeLa cells were in prophase and contained brightly staining kinetochores; 80% of the cells were in metaphase and contained dimly staining kinetochores (95 cells examined; staining intensity was judged from the peak pixel values in unscaled deconvolved images). After nocodazole treatment for 15 min, the fraction of cells with brightly staining kinetochores remained constant despite the total loss of chromosome-microtubule attachment ($n = 215$ cells; data not shown). We conclude that the low levels of hBub3 staining observed on microtuble-attached metaphase kinetochores relative to kinetochores in nocodazole-treated cells reflect the presence of less Bub3 on the former and are not a simple consequence of masking Bub3 epitopes by microtubules. Recently, we have been able to confirm this interpretation in 3T3 cells that contain retroviral constructs expressing low levels of green fluorescent protein-Bub3 fusion protein (K.B.K. and P.K.S., unpublished observations).

In HeLa cells arrested at mitosis using nocodazole for 18 hr, Bub3 is found on chromosomes in a distinctive double-crescent structure (Fig. 3*G*). If we assume that various shapes in

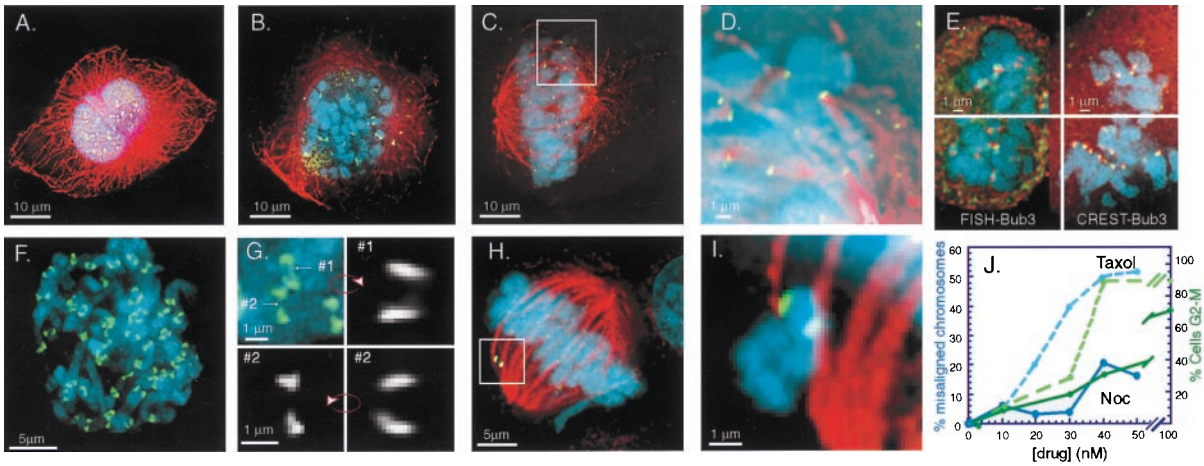

FIG. 3. Immunolocalization of hBub3 in HeLa cells. Representative optical sections from each deconvolved data set are presented with Bub3 in green, tubulin in red, and DNA in blue. (*A*) An early prometaphase cell chosen from an asynchronous culture. (*B*) Late prometaphase cell. (*C*) Metaphase cell. (*D*) An enlarged view of the highlighted square in *C*. (*E*) Images of cells costained by using mBub3 antisera and either alpha-satellite fluorescent *in situ* hybridization (FISH) (*Left,* FISH red, Bub3 green) or CREST antikinetochore sera (*Right,* CREST red, Bub3 green). (F) Cell after treatment for 18 hr with a high concentration (1 μM) of nocodazole (tubulin is depolymerized by this treatment). (G) Bub3 forms a distinct structure on kinetochores. Two enlarged images of kinetochores from the nocodazole-treated cell in *F*, marked 1 and 2, were magnified and then rotated about their long axes to show their characteristic crescent-like structure. (*H*) Cell after treatment for 20 hr with a low concentration (20 nM) of taxol. Two bright Bub3 signals are visible on a lagging chromosome that projects out of the page. (*I*) Magnified view of lagging chromosomes from the metaphase cell in *H*. (J) Percentage of cells with Bub3-positive lagging chromosomes after 20-hr treatment with 0–50 nM taxol (dashed blue line) or nocodazole (solid blue line). Percent of cells treated that were arrested in G_2/M as judged by FACS analysis (taxol, dashed green line; nocodazole, solid green line).

micrographs represent different angular views of a common structure, then Bub3 at kinetochores forms large complexes in which two *ca.* 0.8-μm diameter discs, one on each sister chromatid, are linked by a thin-interchromatid connection. Bub3 appears to extend along the entire face of the kinetochore and even may span a region between the sisters. By comparing, on immunoblots, the amount of hBub3 in HeLa cells extracts with a purified recombinant mBub3 standard, we estimate that there are about 60,000 copies of Bub3 per cell (this corresponds to an intracellular concentration of 200 nM; data not shown). Thus, each kinetochore-bound Bub3 complex may contain up to 1,000 molecules of Bub3. Perhaps Bub3 forms an extended chromosome-bound scaffold that recruits Bub1 to kinetochores (22).

Bub3 Is Present at Low Levels on the Kinetochores of Metaphase Chromosomes. Waters *et al.* (13) have reported that in PtK2 cells Mad2 is present on unattached kinetochores but absent from attached kinetochores. We have not detected Bub3 on microtubule-attached metaphase PtK2 kinetochores. However, in deconvolved 3D reconstructions of mitotic HeLa cells we can see that Bub3 is present on aligned chromosomes at the extreme ends of the microtubules, the presumed site of kinetochores (Fig. 3*D*). Quantitative analysis suggests that the amount of Bub3 at kinetochores is 3- to 5-fold lower on kinetochores in metaphase than in prophase or prometaphase (as judged either by peak or average pixel intensity). Thus, we conclude that the highest levels of kinetochore-associated Bub3 are found in prometaphase, and that a lower but significant amount of Bub3 persists on kinetochores until the end of anaphase.

Presence of Bub3 at High Levels on the Kinetochores of Lagging Chromosomes. Gross perturbations of the microtubule cytoskeleton, such as those produced by high levels of nocodazole, are unlikely to occur during normal cell division and the mitotic checkpoint does not exist solely to respond to complete spindle disruption. Instead, it is thought that the checkpoint functions to delay cell cycle progression when unattached or lagging chromosomes are present. To examine Bub3 localization in cells with such misaligned chromosomes, we treated HeLa cells with very low levels (1–100 nM) of the microtubule poisons taxol and nocodazole. At high concentrations, taxol stabilizes microtubules and nocodazole disrupts microtubules, but at nanomolar concentrations, the two drugs appear to have similar and subtle effects: both disrupt polymer dynamics at the (+) ends of microtubules and increase the number of lagging chromosomes (26). After 20 hr of exposure to low concentrations of drug (taxol $\leq$50 nM or nocodazole $\leq$30 nM), the gross architecture of the spindle was unaltered (see, for example, Fig. 3*H*), but there was a dramatic increase in the number of cells with lagging chromosomes (Fig. 3 *I* and *J*). The average number of lagging chromosomes per cell also increased. In these cells, correctly aligned chromosomes had low levels of Bub3 staining, indistinguishable from the levels of Bub3 on metaphase chromosomes in untreated cells. In contrast, the lagging chromosomes stained very brightly for Bub3, reminiscent of prometaphase chromosomes (Fig. 3*I*). Thus, when mitosis is subtly disrupted over a prolonged period with microtubule poisons, the number of chromosomes that have not correctly aligned on the spindle increases, and these lagging chromosomes selectively retain high levels of Bub3.

Regulating the Amount of Bub3 on Kinetochores. What controls the level of Bub3 at the kinetochores of lagging chromosomes? One possibility is that Bub3 is recruited to the kinetochores of sister chromatids that are not under tension. To test this idea, we treated cells briefly with high concentrations of taxol under conditions that abolish tension in the spindle but do not disrupt chromosome-microtubule attachment. To judge whether pairs of sister chromatids were under tension, we measured the distance between the kinetochores (Fig. 4*A*). In a typical experiment with HeLa cells, we estimated that the kinetochore-to-kinetochore distance, as judged from adjacent Bub3 signals, was 0.75 μm $\pm$ 0.12 (n = 20, Fig. 4*A*, green data points) in prophase, 1.3 μm $\pm$ 0.2 (n = 25, Fig. 4*A*, blue data points) in metaphase, and 0.68 μm $\pm$ 0.1 (n = 22) after a 2-hr treatment with 1 μM nocodazole (data not shown). These values are not dissimilar to values obtained by Shelby *et al.* (27) for live HeLa cells, but, in our experiments fixation introduced greater experiment-to-experiment variability. We synchronized cells in S phase, released them into fresh medium until they were largely mitotic, and then treated them with high concentrations of taxol (10 μM) for 30 min. In taxol-treated cells with a metaphase-like morphology, the kinetochore-to-kinetochore distance had decreased from the metaphase separation of 1.3 μm to 0.60 $\pm$ 0.2 μm (n = 20, Fig. 4*A*, red data points) showing that tension in the spindle had been largely abolished as a consequence of the disruption of microtu-

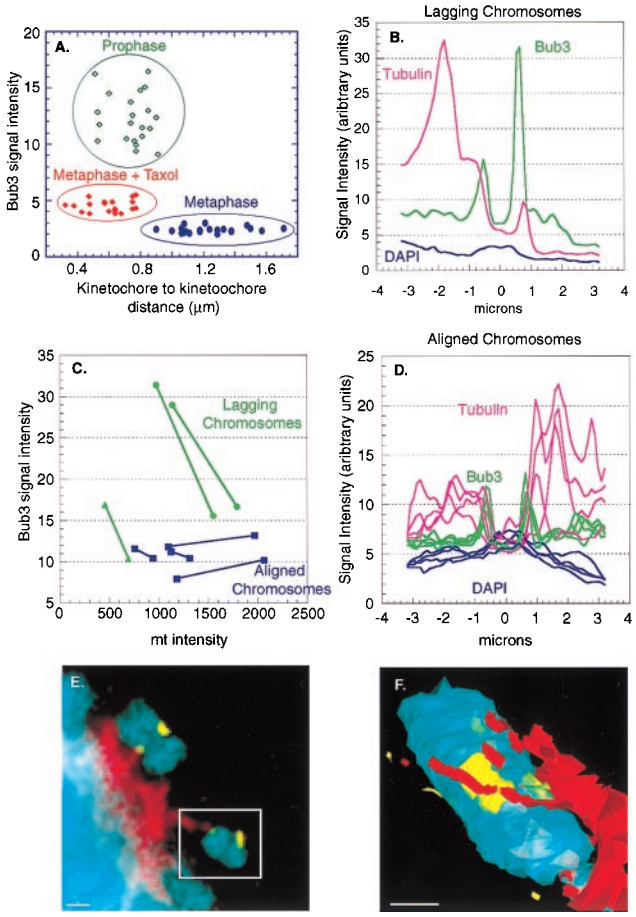

FIG. 4. Relationship between Bub3 signal strength and microtubule attachment. (*A*) Plot of Bub3 signal intensity versus kinetochore-to-kinetochore distance for an untreated prophase cell (green points), a metaphase cell (blue points), and a cell with metaphase morphology treated for 30 min with 10 μm taxol (red points). Peak signal intensities in the Bub3 channel are reported without background correction. (*B*) Relationship of Bub3, tubulin and DNA (DAPI, 4′,6-diamidino-2-phenylindole) fluorescent intensities along a line normal to the kinetochores of a lagging chromosome. (*C*) Plot of peak Bub3 staining intensities versus microtubule intensities for three lagging and four aligned chromosomes by using data derived from the graphs in *B* and *D*. (*D*) Relationship of Bub3, tubulin, and DNA intensities for four aligned chromosomes. (*E*) HeLa cell treated with 20 nM taxol for 16 hr showing two lagging chromosomes bound to what appear to be astral microtubules. Chromosomes stain blue, microtubules red, and Bub3 yellow (a pseudo-color substitute for FITC). (*F*) Model of a lagging chromosome from *E*, showing what appears to be a lateral attachment to a microtubule. Transparent modeling of the chromosome allows the smaller, spindle pole-proximal Bub3 signal to be seen through the DNA.

bule dynamics. Significantly, the rapid removal of tension from spindles was associated with only a relatively small increase in the amount of kinetochore-associated Bub3, as judged by quantitating pixel intensities in deconvolved images (Fig. 4*A*, compare red and green data points). However, as expected from the data presented in Fig. 3, the sustained (greater than 2 hr) treatment of cells with high concentrations of taxol led to spindle collapse, the generation of unattached kinetochores, and the eventual recruitment of high levels of Bub3 to all kinetochores (data not shown). We conclude from these data that Bub3 levels at kinetochores do not rise rapidly in response to the abolition of spindle tension and that kinetochores on unattached chromosomes have much higher Bub3 staining than kinetochores on relaxed chromosomes.

A second way in which the level of kinetochore-associated Bub3 might be controlled is by the extent of microtubule attachment. To explore this possibility, we looked for sister chromatids in which one kinetochore was associated with intense microtubule staining while the other kinetochore had low staining (28). Each human kinetochore can bind up to 20 microtubules, and differences in the levels of kinetochore-associated microtubule staining presumably reflect differences in the numbers of attached microtubules. We examined carefully five lagging chromatids and found that in all cases there was an inverse correlation between the amount of tubulin staining and the amount of Bub3 staining on the two sister kinetochores (this was done by comparing peak signal intensities in the green Bub3 and the red tubulin channels along a line normal to the chromosomes Fig. 4*B*, and green lines in Fig. 4*C*; data not shown). In aligned chromosomes in contrast, tubulin staining was much stronger and there was no obvious correlation between the levels of Bub3 and tubulin (Fig. 4*C* blue lines and *D*). This semiquantitative analysis was consistent with the morphology of the chromosomes (Fig. 4 *E* and *F*). These data imply that the levels of Bub3 on kinetochores vary with the number of kinetochore-bound microtubules rather than with the amount of tension on the sister chromatids.

DISCUSSION

To begin to elucidate the nature of the signal that delays mitosis in response to the presence of incorrectly aligned chromosomes, we and others have isolated murine and human homologues of yeast genes shown genetically to be required for mitotic checkpoint function. The degree of conservation among yeast and animal cell mitotic checkpoint proteins is striking. Human or mouse proteins 15–40% identical to yeast Mad1–3, Bub1, and Bub3 now have been described (8, 11, 12, 14, 29). Those mammalian proteins that have been examined (Mad1, Mad2, Bub1, and Bub3) appear to localize to kinetochores, and it seems likely that the yeast checkpoint proteins also will be found at kinetochores. Thus, mitotic checkpoint proteins are much more highly conserved during evolution than the DNA binding and core components of kinetochores (30).

Similarity Between Bub3 and Proteins Involved in Nuclear-Cytoplasmic Transport. The *Bub3* gene is part of a small family. As previously noted, budding yeast *Bub3* is approximately 50% identical to *Gle2*, a gene involved in nuclear transport whose fission yeast homologue is Rae1 (21). Database searches using Bub3 and Rae1 from various organisms reveal a two-protein gene family in yeast, *Aspergillus nidulans*, *Drosophila*, *Caenorhabditis elegans*, humans, and mice. Intriguingly, mBub3 clone is not significantly more similar to Sc-Bub3 (29% identity) than to Sp-Rae1 (30% identity). Indeed, as a set, the Rae1 and Bub3 proteins across all species are about 30% identical to each other. However, phylogenetic analysis suggests that Bub3 and Rae1 homologues represent two distinguishable sets of proteins (Fig. 1).

In all species that have been examined, Rae1 and Bub3 contain four WD40 motifs, but the region of similarity between the two proteins extends well beyond the WD40 domains. Crystallographic studies of heterotrimeric G-proteins show that WD40 domains fold into antiparallel β-sheets and that seven of these sheets combine to form a compact β-propeller structure (31–33). Bub3 probably contains sequences that are not recognizable as WD40 motifs but that fold to form propellers in the structure. What is the significance of the homology between Rae1 and Bub3? It has been suggested that fission yeast *rae1* is involved in the import into the nucleus of proteins required for mitosis (34). Human and *Xenopus* Mad2, while completely dissimilar in sequence to Bub3, are found along the nuclear envelope in interphase cells and at kinetochores only in mitosis (11, 12). Thus, there may be a fundamental connection between the nuclear envelope, the machinery of nuclear pores, and the proteins that control the mitotic checkpoint.

Association of Bub1 and Bub3. To look for interactions among mammalian checkpoint proteins, we have expressed them in recombinant form in baculovirus-infected insect cells. We find that mBub3 associates, apparently quite tightly, with mBub1. mBub3-associated mBub1 is active as a kinase and exhibits a high level of autophosphorylation. Yeast Bub3p previously has been shown to associate with yBub1, suggesting that there are important similarities between the yeast and mouse Bub proteins. In preliminary experiments we have found that hBub1 and hBub3 also are associated in HeLa cell extracts. Moreover, hBub3 appears to form several different types of complexes, as judged by gel filtration chromatography. The smallest of these complexes is the right size for a hBub3 monomer, but the largest appears larger than expected for a hBub1-hBub3 heterodimer. Although incomplete, these observations suggest that hBub1 and hBub3 may stably associate with additional proteins (K.B.K. and P.K.S., unpublished observations). Among these we expect to find the Bub1-related kinase hBubR1 (35, 36).

By comparing, on immunoblots, the amount of Bub3 in HeLa cell extracts with a purified recombinant Bub3 standard, we estimate that there are 1,000 or more copies of Bub3 per kinetochore. Consistent with this estimate, micrographs reveal that Bub3 may be present in very large structures on sister chromatids. Our anti-Bub1 antibodies are 20-fold lower in affinity than our Bub3 antibodies, precluding accurate measurement of mBub1 levels, but it seems that there is significantly less Bub1 in cells than Bub3 (22). The C-shaped Bub3 complexes we observe are similar to the structures observed with antibodies directed against CENP-E, a kinetochore-associated microtubule motor (37). Thus, Bub3 appears not only to be involved in checkpoint signaling, but also to be a major component of kinetochores.

Mechanisms of Checkpoint Signaling. Why is Bub3 present at high levels on unattached and lagging chromosomes, but not on correctly aligned chromosomes? Nicklas and Li (3) have shown that the activity of the mitotic checkpoint is regulated by the imposition of tension on sister kinetochores (3). This hypothesis makes sense because tension can be generated only when sister chromatids have correctly bound to microtubules that emanate from both spindle poles. Tense and relaxed kinetochores appear to differ from each other in their chemical composition, as judged by immunostaining using antibodies against the 3F3 phosphoepitope (38, 39). However, two pieces of data suggest that it is the number of kinetochore-associated microtubules and not the presence of tension that regulates Bub3-kinetochore association. First, even when spindle tension is removed by treating cells with taxol, the amount of Bub3 at kinetochores does not immediately rise. Second, the amount of Bub3 on lagging chromosomes can vary at the two sister kinetochores and the kinetochore with less antitubulin staining stains more brightly for Bub3. In examining lagging chromosomes carefully, we are struck by cases in which brightly Bub3-staining kinetochores appear to be making lateral contacts with microtubules (Fig. 4*F*). Our images are near the limit of resolution for light microscopy, but we nevertheless speculate that Bub3 displacement from kinetochores may require

mature end-on contact with microtubules rather than lateral contact.

In a recent paper, Waters *et al.* (13) conclude that the association of Mad2 with PtK2 kinetochores is regulated by microtubule attachment rather than by tension. However, relaxed kinetochores on metaphase chromatids from PtK2 cells selectively stain with 3F3, even though Mad2 cannot be detected (see also ref. 38). If checkpoint proteins have dissociated from microtubule-bound kinetochores on metaphase chromatids, does this mean that the checkpoint proteins do not play a role in tension sensing? We think not. Although PtK2 metaphase chromosomes lack detectable Mad2 and Bub3, it is clear that metaphase HeLa and 3T3 cell chromosomes do contain kinetochore-bound Bub3, albeit at reduced levels. Thus, the complete removal of Bub3 from kinetochores at metaphase cannot be a precondition for passage through the metaphase-anaphase transition. In PtK2 cells, the amounts of checkpoint proteins present on kinetochores at metaphase simply may be below the level that can be detected by immunofluorescence.

One explanation for our findings is that changes in the amounts of checkpoint proteins at kinetochores arise from differences in the numbers of bound microtubules. Early in mitosis, the recruitment of high levels of Mad2, Bub1, and Bub3 to lagging chromosomes occurs concomitant with the assembly of active attachment sites (Fig. 3 *A* and *B*; ref. 40). Perhaps these kinetochore-bound checkpoint proteins play a role in regulating the timing of anaphase even in cells in which mitosis is proceeding normally. In yeast, the checkpoint appears to be essential only during those rare cell divisions in which chromosome segregation goes awry. In animal cells, however, there is considerable evidence that kinetochore-microtubule attachment plays a more general role in regulating the cell cycle (41).

Later in mitosis, during metaphase, checkpoint proteins dissociate from kinetochores. Lagging chromosomes retain high Bub3 levels, presumably because their microtubule attachment sites never mature. We do not yet know why the levels of kinetochore-associated Bub3 fall as mitosis proceeds, but a simple explanation consistent with our data (Fig. 4) is that microtubules directly displace checkpoint complexes. This displacement may cause a gradual attenuation of the checkpoint signal as previously suggested by Murray for the yeast checkpoint (42).

We find it significant that the frequency at which Bub3-positive lagging chromosomes are produced increases dramatically in cells treated with very low concentrations of taxol. Wilson and colleagues (26) have argued that low concentrations represent the pharmacologically important range for taxol, and thus that subtle perturbations in microtubule dynamics may be the basis for taxol's efficacy as a chemotherapeutic. If checkpoint mutations do indeed increase the rate of nondisjunction to potentiate loss of heterogygosity in tumors, perhaps conditions can be found in which those very checkpoint defects sensitize tumor cells to the action of antimicrotubule chemotherapeutics.

We are indebted to Aurora Burds, Frank Gertler, Tony Sinskey, Max Dobles, Arshad Desai, Michelle Beaucher, Peter Jackson, and Caroline Shamu. This work was supported by an Anna Fuller Fund Fellowship (to M.J.M.-E.), a Leukemia Society Special Fellowship (to K.B.K.), the Searle Scholar's Foundation, the Charles Reed Trust, the Howard and Linda Stern Career Development Professorship, and Merck and Co.

1. Murray, A. W. (1992) *Nature (London)* **359,** 599–604.
2. Wells, W. A. E. (1996) *Trends Cell Biol.* **6,** 228–234.
3. Li, X. & Nicklas, B. (1995) *Nature (London)* **373,** 630–632.
4. McIntosh, J. R. & Hering, G. E. (1991) *Annu. Rev. Cell. Biol.* **7,** 403–426.
5. Lengauer, C., Kinzler, K. W. & Vogelstein, B. (1997) *Nature (London)* **386,** 623–627.
6. Rabinovitch, P. S., Reid, B. J., Haggitt, R. C., Norwood, T. H. & Rubin, C. E. (1988) *Lab. Invest.* **60,** 65–71.
7. Nowell, P. C. (1976) *Science* **194,** 23–26.
8. Cahill, D. P., Lengauer, C., Yu, J., Riggins, G. J., Willson, J. K., Markowitz, S. D., Kinzler, K. W. & Vogelstein, B. (1998) *Nature (London)* **392,** 300–303.
9. Li, R. & Murray, A. W. (1991) *Cell* **66,** 519–531.
10. Hoyt, M. A., Totis, L. & Roberts, B. T. (1991) *Cell* **66,** 507–517.
11. Li, Y. & Benezra, R. (1996) *Science* **274,** 246–248.
12. Chen, R. H., Waters, J. C., Salmon, E. D. & Murray, A. W. (1996) *Science* **274,** 242–246.
13. Waters, J. C., Chen, R. H., Murray, A. W. & Salmon, E. D. (1998) *J. Cell. Biol.* **141,** 1181–1191.
14. Taylor, S. S. & McKeon, F. (1997) *Cell* **89,** 727–735.
15. Gorbsky, G. J., Chen, R. H. & Murray, A. W. (1998) *J. Cell. Biol.* **141,** 1193–1205.
16. Li, Y., Gorbea, C., Mahaffey, D., Rechsteiner, M. & Benezra, R. (1997) *Proc. Natl. Acad. Sci. USA* **94,** 12431–12436.
17. Roberts, B. T., Farr, K. A. & Hoyt, M. A. (1994) *Mol. Cell. Biol.* **14,** 8282–8291.
18. Rosenblatt, J., Gu, Y. & Morgan, D. O. (1992) *Proc. Natl. Acad. Sci. USA* **89,** 2824–2828.
19. Kaplan, K. B., Hyman, A. A. & Sorger, P. K. (1997) *Cell* **91,** 491–500.
20. Murphy, R., Watkins, J. L. & Wente, S. R. (1996) *Mol. Biol. Cell.* **7,** 1921–1937.
21. Brown, J. A., Bharathi, A., Ghosh, A., Whalen, W., Fitzgerald, E. & Dhar, R. (1995) *J. Biol. Chem.* **270,** 7411–7419.
22. Taylor, S. S., Ha, E. & McKeon, F. (1998) *J. Cell. Biol.* **142,** 1–11.
23. Bharathi, A., Ghosh, A., Whalen, W. A., Yoon, J. H., Pu, R., Dasso, M. & Dhar, R. (1997) *Gene* **198,** 251–258.
24. Agard, D. A., Hiraoka, Y., Shaw, P. & Sedat, J. W. (1989) *Methods Cell. Biol.* **30,** 353–377.
25. Tuffanelli, D. L., McKeon, F., Kleinsmith, D. M., Burnham, T. K. & Kirschner, M. (1983) *Arch. Dermatol.* **119,** 560–566.
26. Jordan, M. A., Wendell, K., Gardiner, S., Derry, W. B., Copp, H. & Wilson, L. (1996) *Cancer Res.* **56,** 816–825.
27. Shelby, R. D., Hahn, K. M. & Sullivan, K. F. (1996) *J. Cell. Biol.* **135,** 545–557.
28. Hayden, J. H., Bowser, S. S. & Rieder, C. L. (1990) *J. Cell. Biol.* **111,** 1039–1045.
29. Jin, D. Y., Spencer, F. & Jeang, K. T. (1998) *Cell* **93,** 81–91.
30. Hyman, A. A. & Sorger, P. K. (1995) *Annu. Rev. Cell Dev. Biol.* **11,** 471–495.
31. Wall, M. A., Coleman, D. E., Lee, E., Iniguez-Lluhi, J. A., Posner, B. A., Gilman, A. G. & Sprang, S. R. (1995) *Cell* **83,** 1047–1058.
32. Lambright, D. G., Sondek, J., Bohm, A., Skiba, N. P., Hamm, H. E. & Sigler, P. B. (1996) *Nature (London)* **379,** 311–319.
33. Sondek, J., Bohm, A., Lambright, D. G., Hamm, H. E. & Sigler, P. B. (1996) *Nature (London)* **379,** 369–374.
34. Whalen, W. A., Bharathi, A., Danielewicz, D. & Dhar, R. (1997) *Yeast* **13,** 1167–1179.
35. Jablonski, S. A., Chan, G. K., Cooke, C. A., Earnshaw, W. C. & Yen, T. J. (1998) *Chromosoma* **107,** 386–396.
36. Chan, G. K., Schaar, B. T. & Yen, T. J. (1998) *J. Cell. Biol.* **143,** 49–63.
37. Thrower, D. A., Jordan, M. A. & Wilson, L. (1996) *Cell Motil. Cytoskeleton* **35,** 121–133.
38. Gorbsky, G. J. (1995) *Trends Cell. Biol.* **5,** 143–148.
39. Nicklas, R. B., Ward, S. C. & Gorbsky, G. J. (1995) *J. Cell Biol.* **130,** 929–939.
40. Ault, J. G. & Rieder, C. L. (1994) *Curr. Opin. Cell. Biol.* **6,** 41–49.
41. Rieder, C. L., Schulz, A., Cole, R. & Sluder, G. (1994) *J. Cell Biol.* **127,** 1301–1310.
42. Murray, A. W. (1995) *Curr. Opin. Genet. Dev.* **5,** 5–11.
43. Efimov, V. P. & Morris, N. R. (1998) *Genetics* **149,** 101–116.
44. Wu, L., Osmani, S. A. & Mirabito, P. M. (1998) *J. Cell. Biol.* **141,** 1575–1587.
45. Felsenstein, J. (1989) *Cladistics* **5,** 164–166.
46. Neer, E. J., Schmidt, C. J., Nambudripad, R. & Smith, T. F. (1994) *Nature (London)* **371,** 297–300.